

Capacitance transient study of the deep Fe acceptor in indium phosphide

A. Dadgar, R. Engelhardt, M. Kuttler, and D. Bimberg

Institut für Festkörperphysik, Technische Universität Berlin, Hardenbergstrasse 36, D-10623 Berlin, Germany

(Received 18 March 1997)

We present a detailed study of the electrical properties of the deep $\text{Fe}^{2+/3+}$ acceptor in InP by deep-level transient spectroscopy. The Fe acceptor transition has been observed in electron and hole emission in n - and p -type InP. A study of the electron emission signature reveals an electric-field enhancement of the emission rate, which is best explained by a polarization potential model. At 300 K electron and hole capture cross sections of 1.5×10^{-17} and 4×10^{-18} cm^2 were determined, respectively, indicating the Fe acceptor being a recombination center. The capture cross sections were found to be temperature dependent in agreement with a multiphonon emission process with activation energies of 138 ± 13 meV for electron and 161 ± 15 meV for hole capture. Measurements of the $\text{Fe}^{3+/2+}$ electron capture cross section at electric-field strengths above 4×10^4 V/cm reveal an approximately 70 times higher value of 1×10^{-15} cm^2 than without an electric field due to an electric-field-induced lowering of the capture barrier. This increase of the capture cross section is most likely due to a decreased capture barrier for electrons in the L valleys. Since the capture barrier is close to zero when an electric field is applied, the apparent activation energy of $E_C - 0.62$ eV, determined by deep-level transient spectroscopy from the carrier emission in an electric field, has not to be corrected by the zero-field capture barrier energy. [S0163-1829(97)03139-1]

I. INTRODUCTION

Fe is still the commonly used dopant to fabricate semi-insulating (si) InP, a key material for high-speed electronic and optoelectronic devices. Due to its importance in device fabrication and the availability of Fe-doped InP the properties of Fe in InP were widely investigated in the last two decades.¹ The energetic position of this transition metal (TM) has been established to be close to midgap in InP at $E_A(1.3 \text{ K}) = E_V + 0.79$ eV.² A wide understanding of the optical spectra has been obtained¹ but some essential electrical properties, necessary for modeling the transport of InP:Fe, are not understood. Deep-level transient spectroscopy (DLTS) measurements were made by several groups,³⁻⁸ mostly focusing on the $\text{Fe}^{2+/3+}$ electron emission signal, which is easily observed. Slightly differing activation energies and emission signatures are reported. In addition, Babinski, Korona, and Hennel studied the pressure dependence of the emission rates of the Fe center in p - and n -type InP, and observed that the hole emission is strongly pressure dependent and that the electron-capture cross section must be larger than the hole-capture cross section.⁶ Based on photoluminescence experiments Klein, Furneaux, and Henry concluded that the low-temperature hole-capture cross section is smaller than the electron-capture cross section.⁹ Look determined the electron-capture cross section by photoconductivity measurements to 1×10^{-15} cm^2 .¹⁰ Turki, Piccoli, and Viallet postulated from the I - V characteristics of si InP:Fe samples that the electron-capture cross section and emission rate is dependent on the electric-field strength.¹¹

In this work we present a detailed study of the Fe acceptor in InP by DLTS. We have directly measured the electron- and hole-capture cross sections and the electric-field dependence of the electron-capture cross section. Further, the electron emission signature was studied in detail and revealed a field enhancement of the emission rate.

II. EXPERIMENT

For DLTS measurements we used Fe-doped InP samples grown by metal-organic chemical-vapor deposition (MOCVD) and liquid-phase epitaxy (LPE). All MOCVD samples were p^+ -InP-substrate/ p -InP:Zn/ n^+ -InP:Si and n^+ -InP-substrate/ n -InP/ p^+ -InP:Zn or n^+ -InP-substrate/ n -InP/Si/ p^+ -InP:Zn diodes with intentional or unintentional Fe doping of the low p - or n -type doped InP side. The LPE sample used was a p^+ -InP-substrate/ p -InP:Zn/ n^+ -InP:Te sample with an unintentional Fe doping due to a contamination of the source materials. On some samples secondary-ion-mass-spectroscopy measurements (SIMS) were made with an ATOMICA 6500 using an oxygen primary beam.

For DLTS measurements Ohmic contacts were evaporated on the top and bottom of the layers and mesa diodes were fabricated using photolithography and wet chemical etching. To enable optical generation of electron-hole pairs in the highly doped top layer the Ohmic top contact was only covering a small part of the mesa diode ($\sim 6\%$).

DLTS measurements were made with a computer-controlled setup using a Boonton 7200 capacitance bridge and a HP 8115A pulse generator. For optical excitation of charge carriers we used commercially available GaAs, $\text{Ga}_x\text{In}_{1-x}\text{N}$, and GaN light-emitting diodes operating around 940, 560, and 450 nm, respectively. Full transients were recorded and analyzed by computer simulating a boxcar window or by directly evaluating the capacitance change in the isothermal transient data.

III. RESULTS

A. Electron emission in n -type InP:Fe

DLTS spectra of Fe-doped n -type InP samples reveal an electron emission signal around 300 K (Fig. 1). This is the well-known DLTS signal correlated to the $\text{Fe}^{2+/3+}$ transition

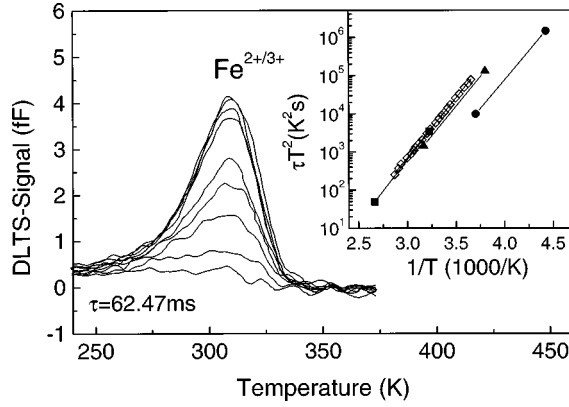


FIG. 1. DLTS spectra of n -type InP:Fe for increasing filling pulse lengths (from bottom to top: 100 ns, 200 ns, 400 ns, 600 ns, 800 ns, 2 μ s, 4 μ s, 10 μ s, and 100 μ s). The inset shows the Arrhenius plot and a comparison with literature values for $\text{Fe}^{2+/3+}$ [\diamond , (this work), \bullet (Ref. 3), \blacktriangle (Ref. 4), \blacksquare (Ref. 5)].

having an activation energy of $(E_V - 0.62 \pm 0.01)$ eV. The electron-capture cross section σ_∞ as obtained from the Arrhenius plot for $1/T=0$ yields 1.3×10^{-14} cm 2 .

Measurements of the field dependence of the emission rate were made on two differently doped n -type InP:Fe samples. In Fig. 2 double-correlation deep-level transient spectroscopy¹² (DDLTS) spectra are shown for different field strengths ranging from 1.6×10^5 to 2.6×10^5 V/cm. In higher n -type doped samples suited for higher electric field strengths a negative DLTS signal can be observed at the low-temperature side. This is caused by the known exchange of Fe and Zn at Fe/Zn interfaces¹³ causing a small electron emission signal from the high-field p^+ -type InP:Zn layer which is nominally undoped with Fe. To avoid the exchange of Fe and Zn at the metallurgical junction the sample used for field strengths up to 2.6×10^5 V/cm was grown with a 75-nm n -type InP:Si spacer layer between the n -type InP:Si+Fe and the p^+ -type InP:Zn layers.

The emission rate for the $\text{Fe}^{2+/3+}$ emission in n -type InP at 300 K increases from 11 s^{-1} at 8.3×10^4 V/cm to 32 s^{-1} at 2.2×10^5 V/cm (Fig. 3). The data can be best explained by a polarization potential of the form $V(r) = -A/r^4$ first described by Lax¹⁴ using $A = q^2 \alpha / 8 \pi \epsilon_0 \epsilon_r^2$ (Ref. 15) and a value of $A = 1.3 \times 10^{-29}$ eV cm 4 . A is here about one order

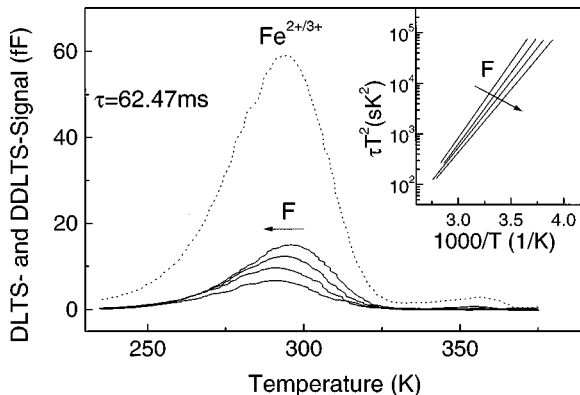


FIG. 2. DDLTS spectra of the $\text{Fe}^{2+/3+}$ emission with field strengths ranging from 1.6×10^5 to 2.6×10^5 V/cm. The inset shows the Arrhenius plots for different field strengths.

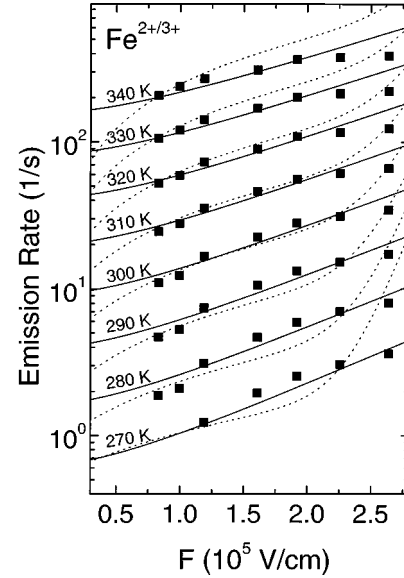


FIG. 3. Electron emission rates vs electric-field strength. A fit with a polarization potential (full line) and a phonon-assisted tunneling model (dashed line) is shown. Fit values are a polarizability α of 2.8×10^{-18} cm 3 for the polarization potential and, for the phonon assisted tunneling model (Ref. 17), $E_A = 620$ meV, $\hbar\omega = 48$ meV, Huang-Rhys parameter $S = 2.4$ and fit parameter $\gamma = 1.2$ (Ref. 18).

of magnitude lower than the value found by Tasch and Sah for the Au center in Si.¹⁶ A fit with a phonon-assisted tunneling model,¹⁷ which is a widely used model to explain emission enhancement from a neutral impurity, does not yield such a good correspondence with the experimental data, especially at higher field strengths (dashed line in Fig. 3).¹⁸ We assign the small deviation between experimental high-field data and the polarization potential to a small negative electron emission signal from the top p^+ -type InP:Zn layer as described above. Obviously the 75-nm “spacing” is not sufficient to prevent completely any Fe to diffuse from the n -type InP:Fe to the p^+ -type InP:Zn layer. However, a negative signal is not actually observed as a negative peak, but it probably overlaps with the positive DLTS peak and does shift the DLTS peak maximum to higher temperatures, or rather seems to lower the emission rate at a given temperature.

The electron capture cross section $\sigma(T)$ was measured by using short filling pulses (>100 ns) in a sample with a low n -type doping level ($N_D < 10^{15}$ cm $^{-3}$). The capture cross section was determined by varying the DLTS filling pulse length and after a Debye tail correction of the data as described in Ref. 19 using

$$\sigma(T) = \frac{1}{\tau_c N v_{\text{thermal}}}, \quad (1)$$

where τ_c is the capture time constant, N the bulk carrier concentration, and v_{thermal} the thermal velocity. σ varies from 1.3×10^{17} to 3.4×10^{17} cm 2 in the temperature range 275–368 K (Fig. 4). The observed capture behavior agrees well with a multiphonon emission process²⁰ with an activation energy of (138 ± 15) meV and a σ_∞ of 1.8×10^{-15} cm 2 (Fig. 4).

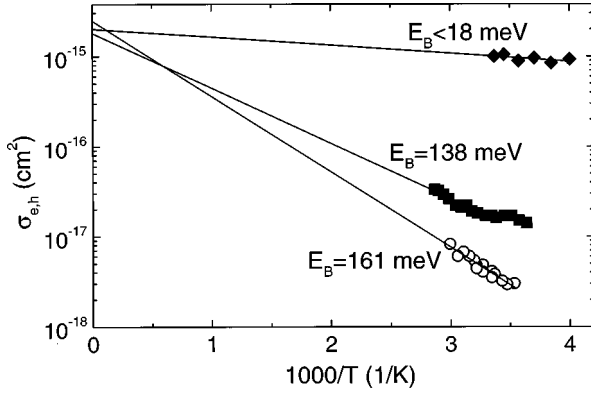


FIG. 4. Electron-capture cross section of the $\text{Fe}^{3+/2+}$ transition without (■) and with (◆) an electric field ($F > 4 \times 10^4$ V/cm) and of the hole-capture cross section without an electric field (○).

To determine the electron-capture cross section in an electric field we used a method first described by Williams²¹ and in more detail by Prinz and co-workers.^{22,23} In the samples used in our work electron-hole pairs are generated in the highly p -type doped top layer using short light pulses. With a partially metallized p^+ -type InP top layer of 800–1000 nm thickness and a sufficiently short light wavelength, only electron-hole pairs several hundred nm from the p^+ - n junction are generated. Some electrons and holes diffuse to the space-charge region and, since there is a barrier for holes, only electrons can be expected to drift through the space-charge region. Subsequently, these electrons can be captured by deep levels. The carrier density N_{DF} in the space-charge region is

$$N_{\text{DF}} = \frac{I}{v_{\text{drift}} A q}, \quad (2)$$

with q the elementary charge, A the area of the diode, I the current, and v_{drift} the drift velocity. Inserted in formula (1), only the measured current I , the area of the diode A , and the capture time constant τ_C are needed to determine the capture cross section $\sigma(T)$,

$$\sigma(T) = \frac{Aq}{\tau_C I}. \quad (3)$$

In contrast to the assumption of Prinz and Rechkunov,²³ v_{thermal} in Eq. (1) was replaced by v_{drift} . At large electric fields as here with $F > 4 \times 10^4$ V/cm v_{drift} can be expected to be larger than v_{thermal} , since v_{thermal} cannot be determined by using $v = \sqrt{3kT/m^*}$ with the effective electron mass at the Γ point, as done by Prinz and Rechkunov.²³ For electrons at such high electric fields m^* is much larger because the electrons get scattered to the L or X valleys. Despite the lower mobility of electrons in the L valleys, v_{drift} for such hot electrons is—already per definition—always larger than v_{thermal} and a second experiment to measure the drift velocity can be avoided.

The electric-field dependence of the capture cross section can be thus easily investigated, since the carriers are captured in the space-charge region of the diode. It is, further, possible to measure the capture cross section even if it is of the order

of 10^{-13} cm^2 or, in samples with a high n - or p -type background doping level, when the minimum filling pulse length of typically 50–100 ns as in conventional DLTS is already too large. Here the carrier concentration is a function of the light intensity, or rather the current.

To exclude errors caused, for example, by the generation of electron-hole pairs in the space-charge region, which can occur when using light with photon energy only slightly above the band gap, we mostly used a green LED with a wavelength around 560 nm. The light penetrates InP here approximately 400 nm ($1/e$ length). More than 90% of the light is absorbed in the 800–1000-nm-thick p^+ layer well before the p^+ / n junction and the current measured is dominated by the electron current. We further used a number of different light intensities, samples, and electric-field strengths and found no difference in our capture data. Since the incident light intensity from the LEDs used was relatively low, the capture time constants were usually of the order or larger than the repetitive emission time constants. We were correcting our capture data taking into account re-emission from the traps during capture and, as far as necessary, the repetition frequency of the measurement. Due to these corrections the experiment is limited to data below 300 K, since a small error in the determination of the emission rate at higher temperatures yields a significant difference in the calculated capture rates.

The observed electron-capture cross sections were approximately 70 times larger than in conventional DLTS measurements where carrier capture occurs during the filling pulse in a region without an electric field. The electron-capture cross section in the temperature range 240–300 K is approximately $(1 \pm 0.2) \times 10^{-15}$ cm^2 at field strengths above 4×10^4 V/cm and shows no field dependence up to a field strength of 1.4×10^5 V/cm (Fig. 4).

B. Hole and electron emission in p -type InP:Fe

For p -type Fe-doped samples DLTS spectra for different filling pulse lengths are shown in Fig. 5(a). A small majority hole emission signal is obtained for short filling pulse lengths, which shows overlap for longer filling pulse lengths by a strongly increasing electron emission signal at a slightly lower temperature. The DLTS spectrum of a sample with different Fe doping in the low p -type doped InP is shown in Fig. 5(b). The region 250 nm close to the metallurgical junction was nominally undoped with Fe [Fig. 5(c)]. In the DLTS spectra obtained from this sample a smaller negative DLTS peak for longer filling pulse lengths can be observed [Fig. 5(b)]. So the negative electron emission signal has its origin in a region close to the metallurgical junction. The remaining negative signal in the second sample is due to the fact that Fe diffuses strongly in p -type InP.¹⁵ Thus always some Fe diffuses to the nominally Fe-undoped region close to the metallurgical junction resulting in the negative DLTS signal. The emission behavior observed in DLTS experiments is quite rare and it will be shown later that it is due to the difference of the electron- and hole-capture cross sections of the $\text{Fe}^{2+/3+}$ transition and not to a signal from the n^+ -type InP layer. However, a determination of the hole-capture cross section in a sample with such an emission behavior is not possible.

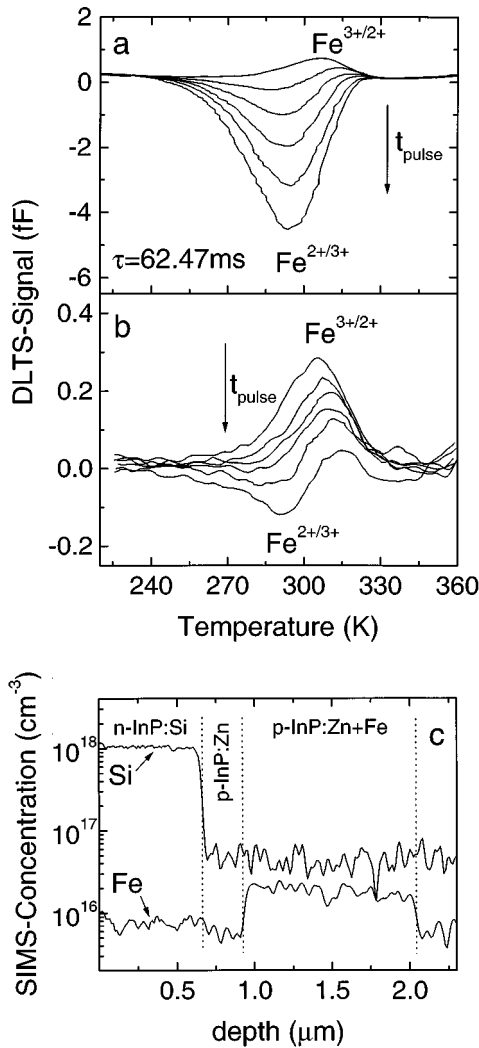


FIG. 5. DLTS spectra for two MOCVD p -type InP:Fe + Zn/ n^+ -type InP:Si samples, which are identical except for the Fe doping profile. The DLTS spectrum in (a) is of a sample with a completely Fe-doped p -type region. The DLTS spectrum in (b) is of a sample with a 270-nm nominally Fe-undoped p -type InP:Zn region close to the metallurgical junction (c). The influence of the Fe content close to the metallurgical junction can be clearly seen in the DLTS spectra for increasing filling pulse lengths ($t_{\text{pulse}} = 200$ ns, 2 μ s, 20 μ s, 200 μ s, 2 ms, 20 ms).

In LPE grown Fe-doped samples the described negative electron emission signal is not observable due to a nonuniform and much lower Fe doping in the p -type layer (Fig. 6). The hole emission signal around 300 K could be clearly identified to be caused by the $\text{Fe}^{3+/2+}$ emission, by comparing the hole emission Arrhenius plot with the electron emission Arrhenius plot (Fig. 6, inset). For a recombination center the emission rates and thus the Arrhenius plots are expected to be the same since the observed emission rate in a DLTS experiment is the sum of the electron and hole emission rates.³⁰ A further proof of the identity of this trap is given by the $\text{Fe}^{2+/3+}$ electron emission signal in DLTS measurements after electron injection. As a result, the positive Fe-related hole emission peak is superimposed by a negative electron emission signal at the same position. The second DLTS peak in Fig. 6 labeled A is related to an unknown contamination of the doping material used. The

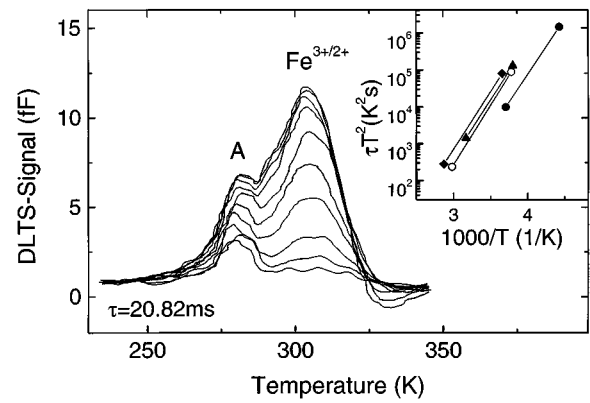


FIG. 6. DLTS spectrum of the LPE-grown p -type InP:Fe sample. Due to a nonuniform Fe doping only the positive $\text{Fe}^{3+/2+}$ hole emission peak is observed. Peak A is due to an unknown contamination of the doping source. The $\text{Fe}^{2+/3+}$ emission peak is increasing with increasing filling pulse time ($t_{\text{pulse}} = 2$ μ s, 4 μ s, 10 μ s, 20 μ s, 40 μ s, 100 μ s, 200 μ s, 400 μ s, 2 ms, 10 ms). The inset shows the hole emission Arrhenius plot (\circ , $\text{Fe}^{3+/2+}$) in comparison to electron emission Arrhenius plots for $\text{Fe}^{2+/3+}$, [\blacklozenge (this work), \blacktriangle (Ref. 4), \bullet (Ref. 5)].

$\text{Fe}^{2+/3+}$ hole-capture cross section could be determined from this sample to vary from 3×10^{-18} to 7.2×10^{-18} cm^2 in the temperature range 284–334 K. The data are in agreement with a multiphonon emission process²⁰ with a capture barrier of $E_B = 161$ meV. The value for σ_∞ determined from the fit is 2.5×10^{-15} cm^2 . Unfortunately no measurement of the field dependence of the hole emission signal could be made, since, for the LPE grown sample without the negative electron emission signal, the residual hole concentration was very low (9×10^{14} cm^{-3}). In higher doped samples suited for such measurements the electron emission signal would dominate the DLTS spectrum as in the MOCVD-grown samples. Also, a determination of the hole-capture cross section at high electric-field strengths with the method described for electron capture was not possible. However, we could determine if the hole-capture cross section σ_p is smaller or larger than the electron capture cross section σ_n . Using a blue GaN LED that mostly generates a hole current in the junction, no hole emission peak could be observed and only a small electron emission signal appears, probably due to the very few electrons that are still generated in the depletion region. In a second experiment, with a GaAs LED, both electrons and holes are generated in comparable concentration in the depletion region and an electron emission peak is observed. Considering the fact that $c_n = \sigma_n n$ and $c_p = \sigma_p p$, where c_n and c_p represent the respective electron- and hole-capture rates, one can determine if σ_p is larger or smaller than σ_n . In the first experiment the electron concentration n must be smaller than the hole concentration p whereas for the second experiment $n \approx p$. Since in both cases no hole emission signal is observed and only a strong electron emission signal is seen in the second experiment, σ_p must be smaller than σ_n in an electric field. Otherwise, if $\sigma_p \geq \sigma_n$ a hole emission signal should be observed in both experiments.

IV. DISCUSSION

Since the Fe level in InP is known to be the 2+/3+ mid-gap acceptor level, attracting positively charged carriers, one

could expect a large hole and a small electron-capture cross section. For example, the $Ti^{3+/4+}$ midgap donor in InP, which can be expected to attract electrons, was found to have an electron-capture cross section nine orders of magnitude larger than the hole-capture cross section.²⁴ In contrast to that, the hole-capture cross section of the Fe acceptor in InP is found to be smaller than the electron-capture cross section. Qualitatively this observation was already made by Babinski, Korona, and Hennel, and Klein, Furneaux, and Henry.^{8,9} However, the values of Klein, Furneaux, and Henry for the electron- and hole-capture cross sections determined from time-dependent photoluminescence measurements are about one order of magnitude larger than ours. It can be excluded that the error in our measurements is so large, that the values must indeed be a factor of 10 larger. Since we could very exactly determine the sample parameters net carrier concentration and the temperature and capture time constants necessary to calculate the capture cross section [see formula (1)], it is most likely that the values of Klein, Furneaux, and Henry are too large. However, the ratio of the zero-field electron- and hole-capture cross sections we found to be about 25, which corresponds to the low-temperature ratio found in the work of Klein, Furneaux, and Henry.⁹ Babinski, Korona, and Hennel showed that the hole-capture cross section increases and gets larger than the electron-capture cross section when applying uniaxial stress: In p -type InP:Fe they observed a smaller DLTS signal than one would expect from the electrically active Fe concentration, and only when applying pressure the DLTS peak increased. They determined that the ratio of the electron- and hole-capture cross sections is about 30 around 300 K.⁸ This is in agreement with our results on p -type InP:Fe where the amplitude of the DLTS peak corresponds to approximately 1% of the Fe concentration as determined by SIMS. We performed numerical simulations of a diode structure as used in our experiments. In these simulations the electron and hole concentrations in the space-charge region of a p/n^+ diode are calculated including the free-carrier Debye tail. First of all, the population of the deep level is determined at reverse bias and then for applying a filling pulse of defined length taking into account electron and hole capture and reemission processes. The population shown in Fig. 7 is the trap population in thermal equilibrium and at the end of filling pulses of different lengths when the reverse bias is reapplied. Our simulations clearly demonstrate that the strong negative electron emission peak in p -type InP:Fe is due to electron capture and reemission in the p -type region close to the metallurgical junction (Fig. 7). This result agrees with the conclusions drawn from DLTS spectra obtained from the two different p -type InP:Fe MOCVD samples (Fig. 5) where, in the sample with a lower Fe concentration close to the metallurgical junction, the negative electron emission signal in the DLTS spectra is smaller. The shift of the negative electron emission signal, which is originating in the high-field region of the diode, is due to the field-induced emission enhancement of the $Fe^{2+/3+}$ electron emission. For these simulations the values for the capture cross section for the field-free case were applied since the hole capture occurs in the field-free region and the ratio of the zero-field capture cross sections is important to explain the small hole emission DLTS peak observed. The electron capture, however, occurs in the high-

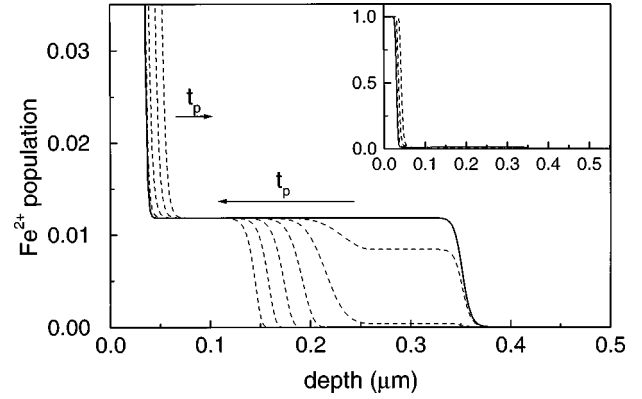


FIG. 7. Simulation of the Fe^{2+} occupation in the p -type InP:Fe sample of Fig. 5(a). The hole-capture cross section is lower than the electron-capture cross section, thus even in p -type material only 1% of the Fe centers in the capture and emission region are in the Fe^{3+} charge state while the rest remains in the Fe^{2+} charge state, resulting in the small DLTS hole emission signal in Fig. 5. Another important and unusual consequence of the electron- and hole-capture cross section ratio is the electron emission region close to the metallurgical junction causing the negative DLTS signal for longer filling pulse lengths (full line, equilibrium; dashed lines, after filling pulses of $t_{pulse} = 200$ ns, 2 μ s, 20 μ s, 200 μ s, 2 ms, 20 ms).

field region of the space-charge region, but it makes no difference if the electron-capture cross section is of the order of 10^{-17} – 10^{-15} cm^2 to model our results, since we would observe the electron emission signal for both values of the capture cross section. By comparing the increase of the capacitance signal with increasing filling pulse length for both values of the electron-capture cross section, we concluded that the electron-capture cross section is indeed larger than 10^{-17} cm^2 in an electric field. It can also be shown that the electron emission signal described here can only be observed in bipolar diodes. In Schottky diodes, which are difficult to fabricate on InP, the electron emission signal is much weaker and appears only for very long filling pulse lengths, because of the lower electron concentration close to the metallurgical junction.

The capture barriers in the field-free case, determined to 138 meV for electron and 161 meV for hole capture, are in good agreement with a multiphonon emission process.²⁰ From these relatively large values one can assume a small perturbation of the InP lattice vibrations close to the Fe acceptor and thus a small displacement of the energy parabolas in the configuration-coordinate scheme (Fig. 8). The values determined for the capture barrier might be lower (E_{BA}) than the real barrier (E_B) since tunneling through the barrier at lower energies is very likely for a configuration with a small displacement of the energy parabolas. Some relative displacement of the parabolas agrees with the results of Bremond *et al.* and Fung, Nicholas, and Stradling, who determined for the $Fe^{2+/3+}$ center in InP a rather small Franck-Condon shift energy (~ 100 meV).^{25,26} In contrast to that Takanohashi and Nakajima determined a Franck-Condon energy shift of zero.²⁷ A Franck-Condon energy shift of zero is, however, impossible because then the capture by a multiphonon emission process, which implies a displacement of the energy parabolas²⁰ and which was already observed by

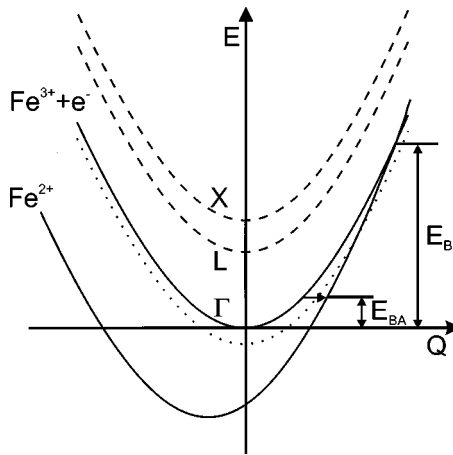


FIG. 8. Configuration coordinate scheme of the $\text{Fe}^{2+/3+}$ transition without an electric field (full line) and in an electric field assuming carrier heating (dashed line) or an electric-field effect (dotted line) (apparent or measured capture barrier E_{BA} , capture barrier E_B).

Klein, Furneaux, and Henry,⁹ is not probable.

Interesting and up to now only scarcely investigated is the difference of the capture cross sections of deep levels with and without an electric field.^{22,23,28,29} For Fe in GaAs such an investigation was reported by Prinz and Rechkunov.²³ They observed a strong field dependence of the $\text{Fe}^{2+/3+}$ capture cross sections in GaAs that increased by about 4 orders of magnitude. The increase for the $\text{Fe}^{2+/3+}$ electron-capture cross section found in InP:Fe by applying an electric field is less than two orders of magnitude. We determined the value to $1 \times 10^{-15} \text{ cm}^2$, which is the same as found by Look from modeling results of photoconductivity measurements.¹⁰ Since a voltage and thus an electric field is applied in photoconductivity measurements the value found by Look must agree with the value for electron capture in an electric field.

For an increase of the capture cross section in an electric field two different models are described in the literature.^{23,31} First of all, in a simple model, carrier heating in an electric field can increase the capture probability since the hot electrons gain a higher energy and consequently the apparent capture barrier is lowered (Fig. 8). The electric-field strength in our samples was higher than $4 \times 10^4 \text{ V/cm}$, resulting in electron energies above the apparent capture barrier, so this process might explain the observed increase of the capture cross section. Also, a dependence of the capture cross section with further increasing electric-field strength cannot be expected when the electron energy is already of the order of or above the capture barrier energy in correspondence with our results. But, as Prinz and Rechkunov already pointed out, this simple model does not take into account that an increase of the electron energy results in a shift of the free-electron parabola to much higher energies up to the L and X valleys where the hot electrons get scattered to. Thus the crossing point of the energy parabolas for the free and bound electron moves towards higher energies and, as a result, the capture barrier will be significantly increased.²³ So the capture cross section should even decrease in an electric field, which was also theoretically evaluated by Abakumov *et al.*³¹ In their semiclassical approach they determined the influence of the charge of a deep center and of carrier heating on the capture

cross section by using a configuration coordinate model and calculating the tunneling probabilities between the bound and free-electron parabolas. They demonstrated that electron heating usually results in a decrease of the capture cross section of a neutral center, as the $\text{Fe}^{3+/2+}$ electron capture transition is. This is, however, in clear contrast to our results.

A second model for the field dependence of the capture cross section by Abakumov *et al.* proposes a change of the energy parabolas in the configuration coordinate scheme.³¹ In this model the parabola for the free electron gets closer to the parabola of the bound electron by applying an electric field. This is the case if the deep level shows a field-enhanced emission rate as the Fe acceptor in InP does.^{31,32} Thus the tunneling probability and, as a consequence of that, the capture cross section increase and the observed capture barrier decreases (Fig. 8). But for Fe in InP this lowering is, especially at field strengths below 10^5 V/cm , negligibly small. So this model cannot explain the increased electron-capture cross section.

Turki, Piccoli, and Viallet observed that the electron-capture cross section increases in a small region of the electric-field strength around approximately 10^4 V/cm .¹¹ This field strength corresponds to the onset of negative differential resistivity at which significant scattering of the electrons from the Γ point to the L valleys occurs. Taking into account our results it is therefore indicated that the capture barrier vanishes or gets much lower for capture of electrons in the L valleys. Consequently, for field strengths below 10^4 V/cm the capture barrier can be expected to increase significantly, in a small region of the electric-field strength, to the value determined in the field-free case. This is not explained by any of the theoretical models discussed in this chapter since all these models suggest that a steady increase of the capture cross section over a wide region of the electric-field strength should be observed. Such behavior would be in contrast to the results of Turki, Piccoli, and Viallet.¹¹ However, at high field strengths, as in our experiments, it is possible that a saturation value of the capture cross section occurs.

The observed field effect of the $\text{Fe}^{2+/3+}$ electron emission accounts for the scatter of the emission data in literature³⁻⁷ and the shift of the electron emission signal with respect to the hole emission in p -type InP:Fe as described in this chapter. The field effect can be best explained by a polarization potential model, which is a reasonable model for a neutral defect.^{14,15} Since a fit with a phonon-assisted tunneling model gave no satisfactory result a strong coupling of the defect to the lattice is not probable. However, there must be a weak coupling, since a multiphonon emission process as observed by us, and a Franck-Condon shift as reported by others,^{25,26} is due to a coupling of the defect to the lattice.²⁰ It is thus very likely that both processes, polarization potential and a weak phonon assisted tunneling process, occur, and the applied electric-field strengths were too low to observe a dominating phonon-assisted tunneling process.

For a determination of the activation energy of a deep level the measured apparent activation energy usually has to be corrected by the capture barrier energy. This would give an activation energy of $E_A \approx E_C - 0.49 \text{ eV}$ for the $\text{Fe}^{2+/3+}$ transition, which is in sharp contradiction with other experimental results.¹ The observed electric-field dependence of the electron-capture cross section explains why, for an accu-

TABLE I. Activation energies and capture cross-section of the deep Fe acceptor level in InP as determined by DLTS measurements.

	E_A from DLTS	σ_∞	Field effect	$\sigma_n(T)$ E_B	$\sigma_p(T)$ E_B	$\sigma_n(T), E_B$ $F > 4 \times 10^4$ V/cm
This work $\text{Fe}^{2+/3+}$	$E_c - 0.62 \pm 0.01$ eV $F \approx 8 \times 10^4$ V/cm	1.3×10^{-14} cm ²	Polarization potential $\alpha = 2.8 \times 10^{-19}$ cm ³	$\sigma_{n_\infty} = 1.8 \times 10^{-15}$ cm ² $E_B = 138$ meV		$\sigma_{n_\infty} = 2e - 15$ cm ² $E_B = 18$ meV
This work $\text{Fe}^{3+/2+}$	$\Delta E = 0.63 \pm 0.03$ eV	6.4×10^{-15} cm ²			$\sigma_{n_\infty} = 2.5 \times 10^{-15}$ cm ² $E_B = 161$ meV	
$\text{Fe}^{2+/3+}$ (Ref. 3)	$E_c - 0.59$ eV	4×10^{-14} cm ²		$> 5 \times 10^{-16}$ cm ²		
$\text{Fe}^{2+/3+}$ (Ref. 4)	$E_c - 0.62$ eV	1.8×10^{-14} cm ²				
$\text{Fe}^{2+/3+}$ (Ref. 5)	$E_c - 0.63$ eV	2×10^{-14} cm ²				
$\text{Fe}^{3+/2+}$ (Ref. 7)	$\Delta E = 0.63 \pm 0.05$ eV	10^{-15} cm ²				
$\text{Fe}^{2+/3+}$ (Ref. 8)	$E_c - 0.65 \pm 0.05$ eV					
$\text{Fe}^{3+/2+}$ (Ref. 8)	$\Delta E = 0.57 \pm 0.05$ eV					

rate determination of the activation energy, the difference of the activation energy, as determined from the Arrhenius plot, and the capture barrier, as determined from a separate standard capture experiment, cannot be used. This is in contrast to the common belief that a capture barrier is increasing the apparent activation energy of a deep level as observed in a DLTS measurement. Since the emission during a standard DLTS measurement occurs in an electric field, the value of the capture barrier at this field strength must be taken into account. Consequently, if this value has not been determined, a correction of the apparent activation energy might be wrong. For the $\text{Fe}^{2+/3+}$ transition, the barrier in an electric field can be determined to be lower than 20 meV. Thus it can be neglected within the error of the DLTS measurement. Additionally if observing both electron and hole emission processes, both processes should be taken into account for an accurate determination of the activation energy.³⁰ Since the difference in the emission processes of a factor of 25 is relatively large, the hole emission process can be neglected.³⁰ So from the low-field electron emission signature one should obtain the activation energy of this level without having a capture barrier correction, only with a little error due to the electric-field effect. The uncorrected value for the low-field activation energy of the $\text{Fe}^{2+/3+}$ emission at 300 K of 620 ± 10 meV is also in good agreement with other values found for the $\text{Fe}^{2+/3+}$ activation energy determined with other methods, which are reported to be around 630 meV at 300 K (see, for example, Ref. 1).

In a recently published photoluminescence study by Söderström *et al.* an electron-capture cross section σ_n of 1×10^{-15} cm² and a hole-capture cross section σ_p of 6×10^{-15} cm² is reported.³³ The value for σ_n agrees with our value in the presence of an electric field. Since the Fe-doped si layers used for the determination of σ_n were epitaxially grown on an *n*-type substrate, it is likely that the samples of Söderström *et al.* have a built-in electric field, bringing their value into agreement with our result. For a determination of σ_p *n*-type samples were used where the Fe doping level was at least a factor of 20 above the known maximum electrically active concentration of approximately 8×10^{16} cm⁻³.¹³ Thus precipitates may strongly influence their results, which were calculated by using σ_n determined in an electric field. In

addition to the problems caused by precipitates and other defects associated with high Fe doping it is not justified to use the σ_n value they measured in an electric field for a determination of σ_p without a field, since these samples are purely *n* type, thus they have no built-in electric field.

V. SUMMARY

We have studied in detail the electrical properties of the deep Fe acceptor in InP (Table I). An investigation of the field dependence of the $\text{Fe}^{2+/3+}$ emission signature shows that the Fe center has a weak field dependence of the emission rate. This field dependence can be best explained by a polarization potential model. For electron capture we found an electric-field dependence of the capture cross section, which increases from 1.5×10^{-17} to 1.0×10^{-15} cm² at 300 K, when increasing the electric-field strength from zero to values above 4×10^4 V/cm. This increase is due to a lowering of the capture barrier of a multiphonon emission process²⁰ from 138 meV close to zero and is most likely correlated to a different capture mechanism for hot electrons in the *L* valleys. For hole emission we observed a much lower DLTS signal than expected from the chemical Fe concentration and in most samples a negative electron emission signal for longer DLTS filling pulse lengths. We have shown that this is due to an about one order of magnitude higher electron- than hole-capture cross section. For an applied electric field we have shown that the electron-capture cross section must be larger than the hole-capture cross section as is the case in the absence of a field.

ACKNOWLEDGMENTS

We are grateful to K. Schatke for assisting with the LP-MOCVD growth and B. Srocka for providing the DLTS simulation program. Parts of this work were funded by the Deutsche Forschungsgemeinschaft and the European Community.

- ¹S. G. Bishop, in *Deep Centers in Semiconductors*, edited by S. Pantelides (Gordon and Breach, New York, 1986).
- ²A. Juhl, A. Hoffmann, D. Bimberg, and H. J. Schulz, *Appl. Phys. Lett.* **50**, 1292 (1987).
- ³P. R. Tapster, M. S. Skolnick, R. G. Humphreys, P. J. Dean, B. Cockayne, and W. R. MacEwan, *J. Phys. C* **14**, 5069 (1981).
- ⁴G. Bremond, A. Nouailhat, G. Guillot, and B. Cockayne, *Electron. Lett.* **17**, 55 (1991).
- ⁵M. Sugawara, M. Kondo, T. Takanohashi, and K. Nakajima, *Appl. Phys. Lett.* **51**, 824 (1987).
- ⁶Tsuginori Takanohashi, Kenja Nakai, and Kazuo Nakajima, *Jpn. J. Appl. Phys.* **27**, L113 (1988).
- ⁷K. Korona, K. Karpinska, A. Babinski, and A. M. Hennel, *Acta Phys. Pol.* **77**, 71 (1990).
- ⁸A. Babinski, K. P. Korona, and A. M. Hennel, in *Proceedings of the 7th Conference on Semi-insulating III-V Materials, Ixtapa, Mexico, 1992*, edited by C. J. Miner, W. Ford, and E. R. Weber (IOP Publishing, Bristol, 1993), p. 253.
- ⁹P. B. Klein, J. E. Furneaux, and R. L. Henry, *Phys. Rev. B* **29**, 1947 (1984).
- ¹⁰D. C. Look, *Phys. Rev. B* **20**, 4160 (1979).
- ¹¹K. Turki, G. Piccoli, and J. E. Viallet, *J. Appl. Phys.* **73**, 8340 (1993).
- ¹²H. Lefevre and M. Schulz, *Appl. Phys.* **12**, 45 (1977).
- ¹³T. Wolf, T. Zinke, A. Krost, H. Scheffler, H. Ullrich, D. Bimberg, and P. Harde, *J. Appl. Phys.* **75**, 3870 (1994).
- ¹⁴M. Lax, *Phys. Rev.* **119**, 1502 (1960).
- ¹⁵P. A. Martin, B. G. Streetman, and K. Hess, *J. Appl. Phys.* **52**, 7409 (1981).
- ¹⁶A. F. Tasch, Jr. and C. T. Sah, *Phys. Rev. B* **1**, 800 (1970).
- ¹⁷S. Makram-Ebeid and M. Lannoo, *Phys. Rev. B* **25**, 6406 (1982).
- ¹⁸A. Dadgar, L. Köhne, M. Zafar Iqbal, and D. Bimberg, in *Proceedings of the 23rd International Conference on the Physics of Semiconductors, Berlin, 1996*, edited by M. Scheffler and R. Zimmermann (World Scientific, Singapore, 1996), p. 2837.
- ¹⁹N. Baber, H. G. Grimmeis, M. Klevermann, P. Omling, and M. Zafar Iqbal, *J. Appl. Phys.* **62**, 2853 (1987).
- ²⁰C. H. Henry and D. V. Lang, *Phys. Rev. B* **15**, 989 (1977).
- ²¹R. Williams, *J. Appl. Phys.* **37**, 3411 (1966).
- ²²V. Ya. Prinz and B. A. Bobylev, *Fiz. Tekh. Poluprovodn.* **14**, 1893 (1980) [*Sov. Phys. Semicond.* **14**, 1097 (1980)].
- ²³V. Ya. Prinz and S. N. Rechkunov, *Phys. Status Solidi B* **118**, 159 (1983).
- ²⁴H. Scheffler, N. Baber, A. Dadgar, T. Wolf, and D. Bimberg (unpublished).
- ²⁵G. Bremond, A. Nouailhat, G. Guillot, and B. Cockayne, *Solid State Commun.* **41**, 477 (1982).
- ²⁶S. Fung, R. J. Nicholas, and R. A. Stradling, *J. Phys. C* **12**, 5145 (1979).
- ²⁷T. Takanohashi and K. Nakajima, *J. Appl. Phys.* **65**, 3933 (1989).
- ²⁸S. H. Koenig, *Phys. Rev.* **110**, 986 (1958).
- ²⁹K. D. Glinchuk and N. M. Litovchenko, *Poluprovodn. Tekh. Mikroelektron.* **28**, 3 (1978).
- ³⁰G. M. Martin, A. Mitonneau, D. Pons, A. Mircea, and D. W. Woodard, *J. Phys. C* **13**, 3855 (1980).
- ³¹V. N. Abakumov, V. Karpus, V. I. Perel, and I. N. Yassievich, *Fiz. Tekh. Poluprovodn.* **22**, 262 (1988). [*Sov. Phys. Semicond.* **22**, 159 (1988)].
- ³²V. N. Agranovich, V. I. Perel, and I. N. Yassievich, in *Nonradiative Recombinations in Semiconductors*, edited by V. M. Agranovich and A. A. Maradudin, Modern Problems in Condensed Matter Sciences, Vol. X (North-Holland, Amsterdam, 1991).
- ³³D. Söderström, S. Marcinkevičius, S. Karlsson, and S. Lourdos, *Appl. Phys. Lett.* **70**, 3374 (1997).